Rare Metal Materials and Engineering
Volume 47, Suppl. 2, August 2018
Cite this article as: Rare Metal Materials and Engineering, 2018, 47(S2): 162-166.

Effect of the Calcination Conditions on Composition and Properties of Mn-Zn Ferrites Prepared by Sol-Gel Method

Sun Yukun[1,2], Li Dongyun[1], Wang Fan[1], Xu Yang[1], Ge Hongliang[1], Yang Hui[2]

[1] China Jiliang University, Hangzhou 310018, China; [2] Zhejiang University, Hangzhou 310027, China

Abstract: A series of Mn-Zn ferrite particles were prepared by a template-assisted sol-gel method and calcined at 773, 973 and 1173 K in air, nitrogen and nitrogen after precalcination at 573 K for 1 h in air. The effects of calcination conditions on composition, morphology and properties of Mn-Zn ferrites were investigated by XRD, TEM, VSM and impedance analyzer. It is found that Mn-Zn ferrites with pure spinel structure, uniform size and morphology are obtained only in nitrogen after precalcination at 573 K for 1 h in air, which provide a new way to prepare Mn-Zn ferrite nanoparticles with spinel structure. The reaction mechanisms of the Mn-Zn ferrites in different calcination atmospheres were analyzed. The calcining temperature has a major influence on the morphology and properties of the Mn-Zn ferrite particles with spinel structure obtained; and with the increasing of the calcination temperature, the particles become larger in size, M_s increases monotonically, H_c first increases and then decreases, T_c decreases monotonically. The permittivity first increases and then decreases, and the dielectric loss shows a sharp rise after slightly decreasing trend with the increasing of frequency.

Key words: calcining conditions; composition; properties; Mn-Zn ferrites

Mn-Zn ferrites are very important soft magnetic materials because of their high magnetic permeability, saturation magnetization, electrical resistivity and low power losses etc[1,2]. They have been widely applied in electronics and electrics fields as deflection yoke rings, microwave devices, antenna rods, electromagnetic interference suppressors, core materials for electronic transformers, etc[3-5]. Sol-gel is a flexible technique to adjust the properties of material by optimizing synthesis parameters, such as hydrolysis time, temperature, precursor concentration and pH of the medium. The advantages of the sol-gel process include high purity, chemical homogeneity, and controllable morphology and grain size[6,7]. Meanwhile, in the preparation process of Mn-Zn ferrites, the calcination conditions (such the calcining temperature and the calcining atmosphere) largely affect the phase identification and magnetic properties of Mn-Zn ferrites obtained, because the calcination conditions affect the valency of Mn and Fe ions.

In this research, Mn-Zn ferrite particles were prepared by a template-assisted sol-gel method and calcined at 773, 973 and 1173 K in air, nitrogen and nitrogen after precalcination. The effects of calcination conditions on composition, morphology and properties of Mn-Zn ferrite were studied.

1 Experiment

The $Mn_{0.5}Zn_{0.5}Fe_2O_4$ nano-particles were prepared by a template-assisted sol-gel method [7]. Iron (III) nitrate nonahydrate, manganese (II) nitrate solution (50%), zinc (II) nitrate hexahydrate, and citric acid, ethanol, and ammonia solution were used for the preparation of the starting sol. The metal nitrates were dissolved in ethanol in required molar ratios to prepare solution A. Citric acid was dissolved in ethanol in a separate vessel to produce Solution B. Then solution B was added into solution A. The resulting mixture was stirred for 4 h and then it was quantitatively titrated by an ammonia solution to a pH of 2. The obtained sol was stirred for 24 h, and then was absorbed by cotton fiber. Sols absorbed by template was dried in an oven at 353 K to get a Mn-Zn ferrite dry gel. Finally, the dry gels were calcined at 773, 973 and 1173 K for 1 h in nitrogen, and precalcined at 573 K for 1 h in air and then calcined at different temperatures for 1 h in nitrogen and air.

The samples of Mn-Zn ferrites are labeled as MZF-N-T, MZF-A-T and MZF-NP-T, in which index MZF designates the composition of $Mn_{0.5}Zn_{0.5}Fe_2O_4$, T represents the calcination temperature in K and that of N, A and NP signify the calcination atmosphere in nitrogen, in air after precalcination and in nitrogen after precalcination, respectively.

The phase composition of the as-prepared samples was

Received date: August 25, 2017
Foundation item: Zhejiang Science and Technology Planning Project (2015C31041)
Corresponding author: Li Dongyun, Ph. D., Associate Professor, College of Materials Science and Engineering, China Jiliang University, Hangzhou 310018, P. R. China, Tel: 0086-571-87676293, E-mail: lidongyun@cjlu.edu.cn

determined using a Bruker D8 advance X-ray diffractometer with Cu Kα radiation (wavelength λ=0.154 18 nm) produced at 40 kV and 27.5 mA, at a scanning rate of 5° min^{-1} and a step of 0.02°. Fourier transform infrared spectroscope (FT-IR) was recorded on a Bruker spectrometer in the range of 400~4000 cm^{-1} using the KBr Pellet method (model Tensor 27, Bruker). The morphology of the as-prepared samples was characterized by transmission electron microscope (TEM, Philips Tecnan F20). The hysteresis loops of the ferrites nano-particles were measured by a vibrating sample magnetometer (LakeShore7407 VSM) equipped with a maximum external magnetic fields of 2 Tesla, from which their saturation magnetization (M_s) and coercivity (H_c) were evaluated. The Curie temperature (T_c) was determined from the dependency of magnetic moment on temperature obtained also by a VSM with an applied magnetic field of 0.5 T in the range of 323~1073 K. The dielectric properties of samples were determined by RF Impedance/Material Analyzer (E4991A, Agilent) at 100 mV from 10 MHz to 1 GHz.

2 Result and Discussion

2.1 Composition analysis

The XRD patterns of Mn-Zn ferrites calcined at 773, 973, and 1173 K for 1 h in air after precalcination are shown in Fig.1a. It is found that the pure $Mn_{0.5}Zn_{0.5}Fe_2O_4$ phase could not be obtained in air after precalcination, and the main phase of MZF-A-T samples are $ZnFe_2O_4$ and a small amount of $MnFe_2O_4$ [8]. It is also found that the samples contain some impurity Mn_2O_3 and Fe_2O_3 phases when the calcination temperature is above 973 K.

The decomposition oxygen pressure of spinel Mn-Zn ferrites can be confirmed by the Morineau formula[9]:

$$\lg P_{O_2}=A-1450/T \quad (1)$$

where, P_{O_2} is decomposition oxygen pressure of spinel Mn-Zn ferrite, T is kelvin temperature, and A is the atmosphere constant.

The decomposition oxygen pressure of Mn-Zn ferrites is lower than that in air, and thus ferrites tend to oxidize at low calcination temperature in air. When the oxygen partial pressure is higher than the ferrite decomposition pressure, the decomposition reaction in ferrites occurs[10],

$$MnFe_2O_4+[O]\rightarrow Fe_2O_3+Mn_2O_3 \quad (2)$$

Fe_2O_3 and Mn_2O_3 precipitate from the Mn-Zn ferrites as separate phases for their body-centered cubic structure. While, Zn easily dissolves in the spinel lattice because Zn has a high solubility[10].

The XRD patterns of MZF-N-T are shown in Fig.1b. It can be seen that the main phase of MZF-N-773 is close to the JCPDS standard card (JCPDS#74-2401), and some small peaks of ZnO are also detected. While the XRD patterns of MZF-N-973 and MZF-N-1173 show that the main phases are the mixture of MnO and FeO with some other phases (ZnO at 973 K, ZnO and Fe at 1173 K). It can be concluded that Mn-Zn ferrites are reduced, which could be ascribed to the strong

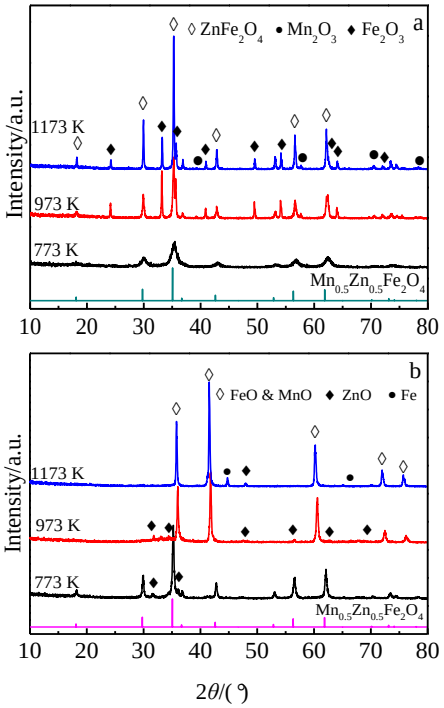

Fig.1 XRD patterns of MZF-A-T (a) and MZF-N-T (b)

reducing atmosphere made up of nitrogen and residual carbon in samples. With the increasing of the calcination temperature, $MnFe_2O_4$ is firstly reduced to MnO and Fe_3O_4 and then $ZnFe_2O_4$ get reduced. Fe_3O_4 starts to be reduced to FeO after all Fe_2O_3 turn into Fe_3O_4. As the samples get further reduced, a part of FeO is thoroughly reduced to Fe.

On the contrary, the XRD patterns of the samples calcined in nitrogen after precalcination (Fig.2a) reveal a single phase spinel structure of Mn-Zn ferrites with no additional peaks from any impurities. Most of the peaks are indexed with the standard pattern reported in JCPDS#74-2401.

The FT-IR spectra curves of Mn-Zn ferrites samples calcined under specific oxygen partial pressure atmosphere in Fig.2b show the obvious characteristic band of $Mn_{0.5}Zn_{0.5}Fe_2O_4$ samples at about 569 cm^{-1}. When the calcination temperature increased, the obvious characteristic band appeared as a stronger band. It is also found that the characteristic absorption bands of the samples show almost no change as calcination temperature changes.

2.2 Microstructure of $Mn_{0.5}Zn_{0.5}Fe_2O_4$

Typical TEM images of $Mn_{0.5}Zn_{0.5}Fe_2O_4$ samples are given in Fig.3. It can be seen from Fig.3 that all samples have uniform size and morphology; there is larger particles size with the increasing of the calcined temperature. The resulting particles have a large size distribution of 20 to 200 nm, which is much larger than the D calculated from the XRD patterns (calculated by Scherrer equation and listed in Table 1) because individual particle consists of several small crystallites.

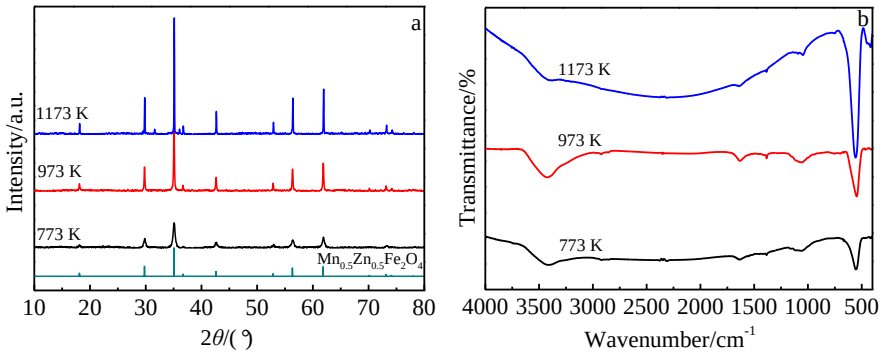

Fig.2 XRD patterns (a) and FT-IR spectra curves (b) of MZF-NP-T

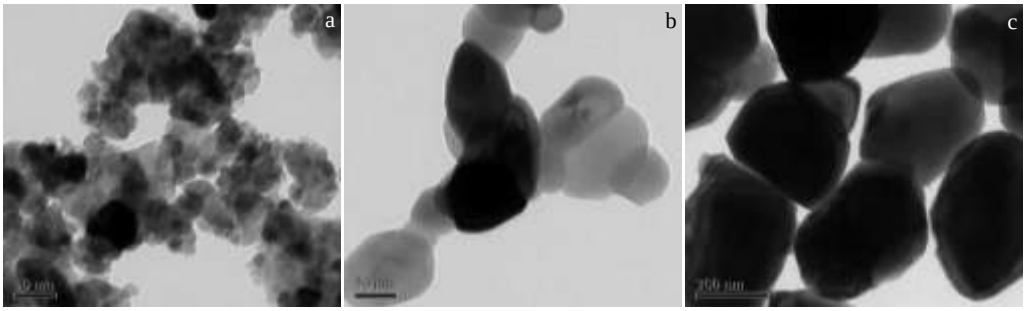

Fig.3 TEM images of $Mn_{0.5}Zn_{0.5}Fe_2O_4$ samples calcined at 773 K (a), 973 K (b), and 1173 K (c)

It can also be seen that the particles agglomerate together extensively in Fig.3a because of the magnetic attraction. As the calcination temperature increased, the initial crystal connecting points gradually grew to form "sintering necks" shown in Fig.3b, and then large particles formed as shown in Fig.3c.

2.3 Magnetic properties

Room-temperature magnetic hysteresis loops for the pure $Mn_{0.5}Zn_{0.5}Fe_2O_4$ samples calcined in nitrogen after precalcination (MZF-NP-T) are shown in Fig.4.

The magnetic properties of MZF-NP-T samples are listed in Table 1. It is found that when the calcination temperatures increased from 773 to 1173 K, the M_s increased from 54.05 (A m^2) kg^{-1} to 87.09 (A m^2) kg^{-1} which could be attributed to the surface effects resulting from the breaking of a large number of exchange bonds for surface atoms (the average crystal size increased from 19.7 nm to 111.3 nm)[11]. And it can also be seen that the H_c values of MZF-NP-773 and MZF-NP-973 are much larger than that of MZF-NP-1173. The sharp decrease from 197.25×80 A/m to 18.33×80 A/m could be explained by the critical grain size (d_{cr})[12].

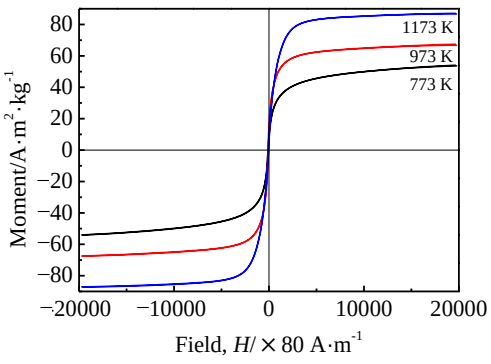

Fig.4 Room-temperature magnetic hysteresis loops for MZF-NP-T

Table 1 Magnetic properties and average crystal size of MZF-NP-T

Sample	MZF-NP-773	MZF-NP-973	MZF-NP-1173
M_s/(A m^2) kg^{-1}	54.05	67.43	87.09
H_c/×80 A m^{-1}	115.09	197.25	18.33
T_c/K	548.58	518.55	512.29
D/nm	19.7	49.4	111.3

The critical grain size (d_{cr}) was estimated by Eq. (3)[13]:

$$d_{cr}=9\varepsilon_p/2\pi M_s^2 \quad (3)$$

Where M_s is the saturation magnetization and ε_p is the surface energy of the domain wall, and value of ε_p is calculated by Eq.(4)[12]:

$$\varepsilon_p=(12k_BT_cK_1/a)^{0.5} \quad (4)$$

Where k_B is the Boltzmann constant (1.38×10^{-16} erg K^{-1}), T_c the Curie temperature, a is the lattice parameter (calculated from $d_{(311)}$ interplanar spacing which is obtained by Bragg

Table 2 Parameters used in estimation of critical grain size

Parameter	T_c/K	$a/\times10^{-8}$ cm	M_s/(A m^2) kg^{-1}	$K_1/\times10^{-4}$ erg cm^{-3}	$\varepsilon_p/\times10^{-5}$ erg cm^{-2}	d_{cr}/nm
MZF-NP-773	548.58	8.48	54.05	1.5	1.64	80.41
MZF-NP-973	518.55	8.48	67.43	1.5	1.59	50.09
MZF-NP-1173	512.29	8.46	87.09	1.5	1.58	29.85

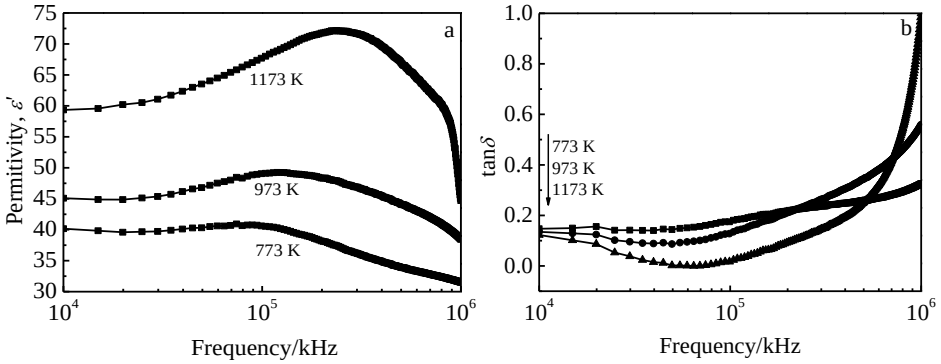

Fig.5 Frequency dependence of permittivity (a) and dielectric loss (b) for samples calcined in specific oxygen partial pressure atmosphere

equation according to the XRD patterns), and K_1 is the absolute value of magnetocrystalline anisotropy constant. The obtained parameter values are listed in Table 2.

As can be seen from Table 1 (average crystal size) and Table 2, the MZF-NP-773 and MZF-NP-973 have smaller crystal size than their critical grain size d_{cr} , while it is larger than that of MZF-NP-1173. As is known, the variety of H_c value are closely interrelated with the calculated d_{cr} value, and below the critical size, the coercivity is much larger than that of samples has a multidomain structure [14]. Therefore, the H_c value in MZF-NP-1173 is smaller than that in MZF-NP-773 and MZF-NP-973, which is reasonable.

According to the classic principle, the H_c of ultrafine grains with a size lower than the d_{cr}, and the H_c behaves proportionally to D^6 as follows [15]:

$$H_c=P_cK_1^4D^6/M_sA \quad (5)$$

Where P_c is a dimensionless factor, A is the exchange constant, and K_1 is magnetocrystalline anisotropy constant. Then, compared with sample MZF-NP-773, a larger H_c in MZF-NP-973 sample which has larger D is reasonable.

2.4 Dielectric properties

The effect of the calcination temperature on the dielectric properties of Mn-Zn ferrites nanoparticles have been studied using impedance analyzer in frequency range of 10 MHz to 1 GHz. The relationship curves between frequency and dielectric constant for spinel Mn-Zn ferrite nanoparticles are shown in Fig.5a and the variation of dielectric loss of the samples with frequency are shown in Fig.5b. It is observed that the permittivity of all Mn-Zn ferrites samples first increases and then decreases. Their dielectric loss shows a sharp rise after slightly decreasing trend with the increasing of frequency. The decrease of permittivity at low frequency with the increasing of frequency can be attributed to the enhancement of ion relaxation polarization. At high frequency, the decrease of dielectric constant and the increase of dielectric loss are related with the disappearance of ion relaxation polarization and the polarization relaxation. The permittivity of Mn-Zn ferrite samples increases, which has been attributed to the effect of heterogeneity of the samples, while their dielectric loss decreases at low frequency and increases at high frequency with the calcination temperature increasing.

3 Conclusions

1) Mn-Zn ferrite particles with spinel structure are synthesized only in nitrogen after precalcination which provideds a new way to obtain Mn-Zn ferrite nanoparticles.

2) Meanwhile, with the increasing of the calcination temperature, M_S exhibits an increasing trend, H_C exhibits an first increasing and then decreasing trend, T_c exhibits a decreasing trend. The permittivity first increases and then decreases, and the dielectric loss shows a sharp rise after slightly decreasing trend with the increase of frequency.

References

1 Meng Y Y, Liu Z W, Dai H C *et al*. *Power Technology*[J], 2012, 229: 270

2 Maleknejad Z, Gheisari Kh, Honarbakhsh Raouf A. *Journal of Superconductivity and Novel Magnetism*[J], 2016, 29(10): 2523

3 Li D Y, Sun Y K, Xu Y *et al*. *Ceramics International*[J], 2015, 41: 4581

4 Wang W J, Zang C G, Jiao Q J. *Journal of Magnetism and Magnetic Materials*[J], 2014, 349: 116

5 Yang L, Xi G X, Liu J J. *Ceramics International*[J], 2015, 41: 3555

6 Sajjia M, Oubaha M, Hasanuzzaman M. *Ceramics International*[J], 2014, 40(1): 1147
7 Lv Hua-nan, Rebrov Evgeny V, Gao Peng-zhao *et al*. *Ceramics International*[J], 2016, 42(1): 7793
8 Dasgupta S, Das J, Eckert J *et al. Journal of Magnetism and Magnetic Materials*[J], 2006, 306: 9
9 Sun Bing. *Thesis for Master Degree*[D]. Nanjing: Nanjing University of Aeronautics and Astronautics, 2014 (in Chinese)
10 Wang Z M. *Production Process and Control Technology of Soft Magnetic Ferrites*[M]. Beijing: Chemical Industry Press, 2013, (in Chinese)
11 Lu A H, Salabas E L, Schüth F. *Angewandte Chemie International Edition*[J], 2007, 46: 1222
12 Li D Y, Sun Y K, Gao P Z *et al. Ceramics International*[J], 2014, 40(10): 16 529
13 Rahman I Z, Ahmed T T. *Journal of Magnetism and Magnetic Materials*[J], 2005, 290-291(2): 1576
14 Yan M, Peng X L. *Magnetism Foundation and Magnetic Materials*[M]. Hangzhou: Zhejiang University Press, 2006 (in Chinese)
15 Xue D S, Chai G Z, Li X L *et al*. *Journal of Magnetism and Magnetic Materials*[J], 2008, 320: 1541

煅烧条件对溶胶凝胶法制备 Mn-Zn 铁氧体的组成及性能的影响

孙玉坤[1,2]，李冬云[1]，王　凡[1]，徐　扬[1]，葛洪良[1]，杨　辉[2]
(1. 中国计量大学，浙江 杭州 310018)
(2. 浙江大学，浙江 杭州 310027)

摘　要：采用模板辅助溶胶凝胶法在不同的烧结气氛和烧结温度下制备出了一系列 Mn-Zn 铁氧体纳米粉体。利用 XRD、TEM、VSM 和阻抗分析仪等对材料的相组成、形貌和电磁性能进行了表征。结果表明，仅有在 573 K 预烧 1 h 后在氮气气氛中煅烧的样品具有尖晶石结构且颗粒大小均匀；这为制备具有尖晶石结构的 Mn-Zn 铁氧体纳米粉体提供了一条新的途径。同时探讨了 Mn-Zn 铁氧体在不同煅烧气氛中的反应机理。此外，煅烧温度是影响尖晶石结构的 Mn-Zn 铁氧体材料性能的一个重要因素，随着煅烧温度的升高，晶粒尺寸逐渐变大，M_s 单调升高，H_c 先升高后降低，T_c 单调降低；随着频率的升高，介电常数呈现先升高后降低趋势，而介电损耗则呈先缓慢下降而后急速升高的趋势。

关键词：煅烧条件；组成；性能；Mn-Zn 铁氧体

作者简介：孙玉坤，男，1990 年生，博士生，中国计量大学材料科学与工程学院，浙江 杭州 310018，电话：0571-87676293，E-mail: lidongyun@cjlu.edu.cn